Molecular Crystals and Liquid Crystals
Publication details, including instructions for authors and subscription information:
http://www.informaworld.com/smpp/title~content=t713644168

Study of Optical Shutter in Cholesteric Phase of a Double Hydrogen-Bonded Ferroelectric Liquid Crystal with Two Chiral Carbons

V. N. Vijayakumar[a]; M. L. N. Madhu Mohan[a]
[a] Liquid Crystal Research Laboratory (LCRL), Bannari Amman Institute of Technology, Sathyamangalam, India

First published on: 20 October 2010

To cite this Article Vijayakumar, V. N. and Mohan, M. L. N. Madhu(2010) 'Study of Optical Shutter in Cholesteric Phase of a Double Hydrogen-Bonded Ferroelectric Liquid Crystal with Two Chiral Carbons', Molecular Crystals and Liquid Crystals, 528: 1, 163 — 177
To link to this Article: DOI: 10.1080/15421406.2010.504651
URL: http://dx.doi.org/10.1080/15421406.2010.504651

Mol. Cryst. Liq. Cryst., Vol. 528: pp. 163–177, 2010

ISSN: 1542-1406 print/1563-5287 online
DOI: 10.1080/15421406.2010.504651

Taylor & Francis
Taylor & Francis Group

Study of Optical Shutter in Cholesteric Phase of a Double Hydrogen-Bonded Ferroelectric Liquid Crystal with Two Chiral Carbons

V. N. VIJAYAKUMAR AND
M. L. N. MADHU MOHAN

Liquid Crystal Research Laboratory (LCRL), Bannari Amman Institute of Technology, Sathyamangalam, India

A novel series of double hydrogen-bonded liquid crystals has been isolated. A hydrogen bond was formed between a nonmesogen chiral ingredient levo tartaric acid (LTA) and mesogenic alkyl benzoic acids (nBA). Thermal and electrical properties exhibited by levo tartaric acid and alkyl benzoic acid (LTA + nBA) are discussed. An interesting feature of the present investigation is the observation of an optical shuttering action in LTA + 8BA hydrogen-bonded complex on application of a predetermined external DC bias voltage. By enhancement of the DC bias voltage the mesogen behaves like an optical shutter; thus, the hydrogen-bonded complex mesogen acts as an effective light modulator. It was noticed that this action of shuttering was reversible, in the sense that when the applied bias voltage is removed the original texture is restored. Experimental results relating to textures, helix, optical intensity profile, dielectric studies, and optical shuttering action are presented. This optical shutter property of the mesogen can be exploited for commercial and display device applications.

Keywords Chemical synthesis; dielectric properties; differential scanning calorimetry (DSC); organic compounds; phase transitions

Introduction

Liquid-crystal (LC) materials refers to the fourth state of matter that possesses the dual property of crystals and liquids. The physical properties exhibited by the liquid crystals such as optical tilt angle, spontaneous polarization, and response times [1–3] govern the utility of these materials in electro-optic devices. Their overall shape [4] (cylindrical) renders them readily viable for surface alignment. In the field of supramolecular LCs, especially in the field of hydrogen-bonded LCs, the influence of a soft-covalent interaction for the thermal stability of phases of device interest is widely [2–14] studied.

The configuration and spread of the hydrogen bonding interaction with regard to the long molecular dipole moment in calamitic LCs along with the corresponding molecular dipole models are reported [5,7,8] to originate from the distinct properties

Address correspondence to M. L. N. Madhu Mohan, Liquid Crystal Research Laboratory, Bannari Amman Institute of Technology, Tamilnadu, Erode (Dt), Sathyamangalam PIN-638 401, India. E-mail: mln.madhu@gmail.com

in the family of hydrogen-bonded liquid crystals (HBLC). A correlation between the chemical molecular structure of the liquid crystal to that of the magnitude of its physical properties will help in designing mesogens of desired properties. The field of systematic studies in the area of LCs is expected to further reveal the truth of microscopic interactions. The growth of order (and crystalline nature) is logically expected to increase with decreasing temperature in these LC materials in their condensed version of matter. These mesogens are reported [15] to possess fast switching activity in the sub-microsecond range, making them candidates for commercial applications.

In the case of HBLCs, the molecular frame possesses [10,16–22] additional soft-covalent interaction. Further, in the case of nonferroelectric and ferroelectric HBLCs, the observed [13,21] variation in device-relevant properties like thermal stability, spontaneous polarization, tilt angle, switching times, etc., are addressed through dipolar and refined dipolar models to vouch for the fact that soft-covalent interaction extends rather inclined to the long molecular dipole moment. The orientation of these dipoles with respect to the chemical molecular structure is one of the reasons for the occurrence of tilted phases.

With our previous experience [23–30] in designing, synthesizing, and characterizing various types of liquid crystals, a successful attempt has been made in characterizing a novel series of double hydrogen-bonded ferroelectric liquid crystal.

In the present communication, a homologous series of ferroelectric HBLC is designed in such a way that the molecule possesses double hydrogen bonding with the chiral ingredient levo tartaric acid moiety. Thermal and electrical characterizations of the various members pertaining to the present series are discussed in detail.

Experimental

Optical textural observations were made with a Nikon polarizing microscope (Japan) equipped with a Nikon (Japan) digital CCD camera system with 5 mega pixels and 2560 * 1920 pixel resolution. The liquid-crystalline textures were processed, analyzed, and stored with the aid of an ACT-2U (USA) imaging software system. The temperature control of the liquid-crystal cell was equipped with an Instec HCS402-STC 200 (USA) temperature controller (Instec (USA)) to a temperature resolution of $\pm 0.1^{\circ}C$. This unit was interfaced to a computer by IEEE-STC 200 (USA) to control and monitor the temperature. The liquid-crystal sample was filled by capillary action in its isotropic state into a commercially available (Instec (USA)) polyamide-buffed cell with 4-μm spacer. The type of the cell used is homeotropic alignment anti-parallel with conductive area of $10 \times 10\,mm^2$ and 120 ohms/sq mm ITO resistance.

The transition temperatures and corresponding enthalpy values were obtained by differential scanning calorimetry (DSC; Shimadzu DSC-60 (Japan)). Fourier transform infrared (FTIR) spectra were recorded (ABB FTIR MB3000 (Canada)) and analyzed with MB3000 software. Light intensity measurements were made with a photo transistor (TSL 252 (USA)) where the sample was placed under crossed polarizers of the Nikon polarizing microscope. The p-n-alkyl benzoic acids (nBA) and levo tartaric acid (LTA) were supplied by Sigma Aldrich (Germany) and all the solvents used were high-performance liquid chromatography (HPLC) grade.

Synthesis of HBLC

As a representative case, the synthesis of levo tartaric acid and octyl benzoic acid (LTA + 8BA) is discussed. LTA + 8BA was synthesized by the addition of 2 mol

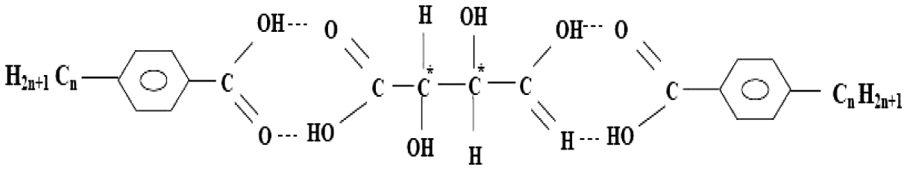

Figure 1. General molecular diagram of LTA + nBA homologous series.

of octyl benzoic acids (8BA) with 1 mol of LTA in DMF. Further, it was subjected to constant stirring for 10 h at ambient temperature of 30°C until a white precipitate in a dense solution formed. The white crystalline crude complex so obtained by removing excess DMF was then recrystallized with dimethyl sulfoxide (DMSO) and the yield was observed to be in the range of 85 to 95%.

A similar procedure was adopted for the synthesis of the other members of the family using ethyl benzoic acid (2BA), propyl benzoic acid (3BA), pentyl benzoic acid (5BA), and heptyl benzoic acid (7BA) with levo tartaric acid. The general molecular structure of the present homologous series of p-n-alkoxy benzoic acids with levo tartaric acid is depicted in Fig. 1, where *n* represents the alkyl carbon number. The yield of the final product was observed to increase with the increment of the alkyl benzoic acid carbon number.

Results and Discussion

Levo tartaric acid and alkyl benzoic acid complexes (LTA + nBA) isolated were white crystalline solids and are stable at room temperature. They are insoluble in water and sparingly soluble in common organic solvents such as methanol, ethanol, and benzene and dichloro methane. However, they show a high degree of solubility in coordinating solvents like DMSO and pyridine. They melt at specific temperatures below 140°C. Further, they show high thermal and chemical stability when subjected to repeated thermal scans performed during polarizing microscopic studies (POM) and DSC studies.

Infrared Spectroscopy (FTIR)

IR spectra of free p-n-alkyl benzoic acid, levo tartaric acid, and their intermolecular hydrogen-bonded ferroelectric complexes were recorded separately in the solid state with KBr at room temperature. As a representative case, the LTA + 8BA hydrogen-bonded complex FTIR spectra is shown in Fig. 2a, and Fig. 2b depicts the FTIR spectra of 8BA. Both are recorded in solid state at room temperature.

The solid-state spectra of free octyl benzoic acid (Fig. 2b) have two sharp bands at 1605 and 1690 cm^{-1} due to the frequency ν(C=O) mode. The doubling feature of this stretching mode confirms the dimeric nature of alkyl benzoic acid at room temperature [21].

Further, in the present hydrogen-bonded complex of LTA + 8BA, a band appearing at 2854 and 2924 cm^{-1} is assigned to the ν(O-H) mode of the carboxylic acid group.

The corresponding spectrum of the solution state (chloroform) shows a strong intense band at 1280 cm^{-1}, suggesting the existence of a monomeric form of benzoic acid. A noteworthy feature in the spectra of the present LTA + 8BA complex is the

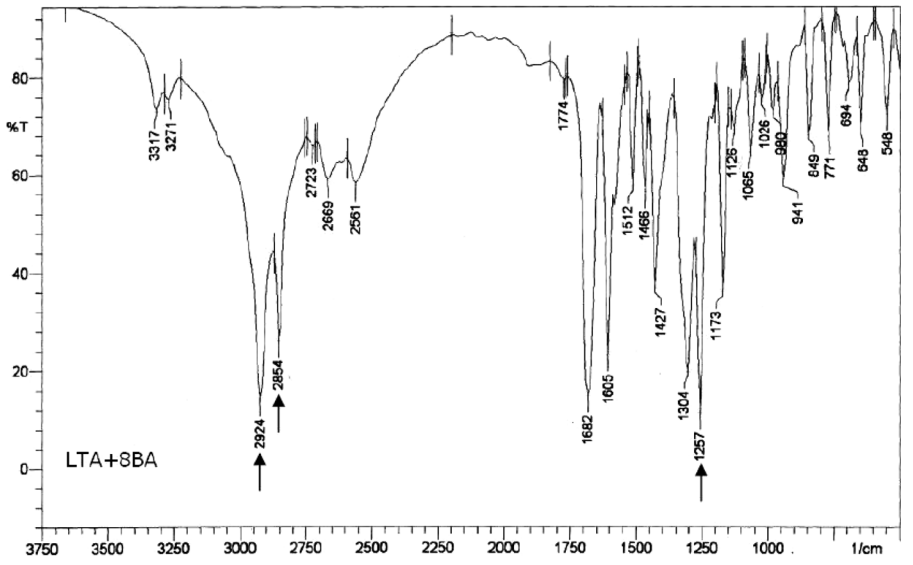

(a)

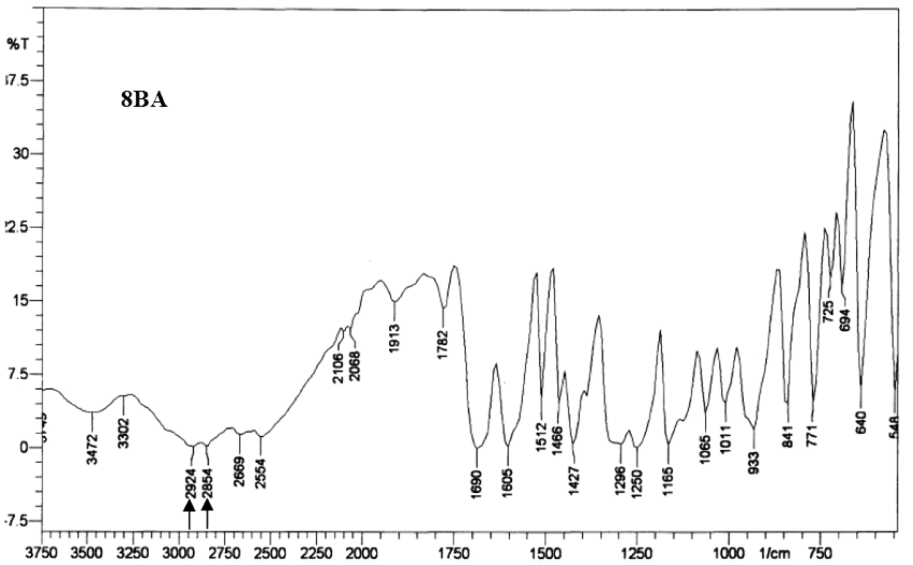

(b)

Figure 2. (a) FTIR spectrum of LTA + 8BA hydrogen-bonded complex and (b) FTIR spectrum of octyl benzoic acid (8BA).

appearance of a sharp band at 1257 cm^{-1}, which is attributed to the doubling nature of ν(C=O) mode of benzoic acid moiety. This clearly suggests that the dimeric nature of the benzoic acid dissociates and prefers to exist in a monomeric form upon complexation.

The formation of a hydrogen bond is evinced through two sharp peaks with wave numbers 2924 and 2854 cm^{-1} observed in the FTIR spectra of the LTA + 8BA

complex (Fig. 2a). It is interesting to notice that these two peaks have much reduced intensities in the octyl benzoic acid (8BA) spectra (Fig. 2b).

Polarizing Optical Microscopic Studies (POM)

The mesogens of the levo tartaric acid and alkxyl benzoic acid (LTA + nBA) ferroelectric homologous series are observed to exhibit characteristic textures [31–34], viz. cholesteric (Ch; fingerprint texture) and smectic G* (multicolored mosaic texture), respectively. The general phase sequence pertaining to LTA + nBA homologous series can be shown as

$$\text{Crystal} \rightarrow \text{Sm G}^* \rightarrow \text{Isotropic} \qquad \text{LTA} + \text{nBA } (n = 2, 3)$$

$$\text{Crystal} \rightarrow \text{Ch} \rightarrow \text{Sm G}^* \rightarrow \text{Isotropic} \qquad \text{LTA} + \text{nBA } (n = 5, 7, 8)$$

Phase Identification

The observed phase variants, transition temperatures, and corresponding enthalpy values obtained by DSC in cooling and heating cycles for the LTA + 8BA complex are presented in Table 1.

DSC Studies of LTA + nBA Homologous Series

DSC thermograms are recorded in heating and cooling cycles. The liquid-crystal sample was crimped in an aluminum cell and heated with a scan rate of 10°C/min and held at its isotropic temperature for one minute to attain thermal stability. The cooling run was performed with an identical scan rate of 10°C/min.

A DSC thermogram of LTA + 8BA is illustrated in Fig. 3. The respective equilibrium transition temperatures and corresponding enthalpy values of this mesogen are listed separately in Table 1. The POM study was in good agreement with the DSC results.

The LTA + 2BA compound is a mono phase variant and the DSC studies reveal one prominent transition in the heating run at 108.9°C with enthalpy value as 61.64 J/g, which is attributed to the crystal-to-melt transition. An isotropic-to-smectic G* phase was observed to be a monotropic transition. In the cooling run the isotropic-to-smectic G* phase transition was observed at 104.9°C. The enthalpy value was merged with the enthalpy value of crystal. Crystallization was observed at 101.6°C with an enthalpy value of 24.96 J/g.

Table 1. Transition temperatures and enthalpy values of various phases in LTA + 8BA

Complex	Phase variance	Technique	Crystal melt	Ch	G*	Crystal
LTA + 8BA	**Ch G***	DSC (h)	99.6 (28.58)	104.9 (1.01)	[a]	
		DSC (c)		101.6 (1.55)	93.5[b]	84.3 (16.2)
		POM (c)		101.9	93.9	84.7

C = Cooling run; h = heating run.
[a]Monotropic transition.
[b]Merged with crystal.

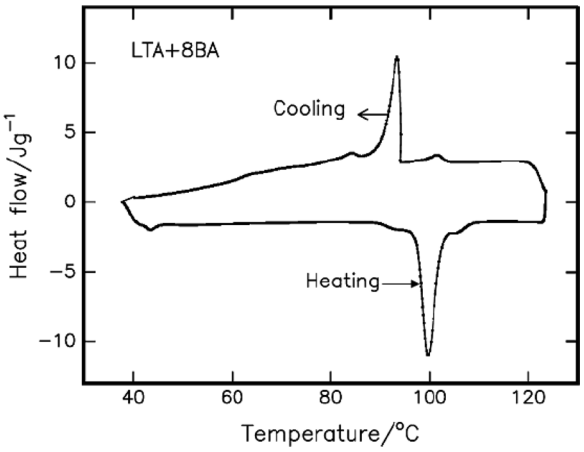

Figure 3. DSC thermogram of LTA + 8BA complex recorded with a scan rate of 10°C/min.

DSC studies of LTA + 3BA indicate that this compound is a mono phase variant with one prominent transition in the heating run at 138.1°C with enthalpy value as 102.63 J/g and is attributed to crystal to melt transition. The isotropic-to-smectic G* phase was observed to be a monotropic transition. In the cooling run the isotropic-to-smectic G* phase transition was observed at 145.1°C and the corresponding enthalpy value was merged with the enthalpy value of crystal. At 135.2°C crystallization was observed with an enthalpy value of 71.25 J/g.

The LTA + 5BA complex is a di-phase variant and DSC studies reveal two prominent transitions in the heating run at 85.7°C and 122.3°C with enthalpy values of 34.24 and 0.86 J/g, which are assigned to crystal-to-melt and melt-to-cholesteric phases, respectively. The cholesteric-to-smectic G* phase was observed to be a monotropic transition in the heating run. In the cooling run the isotropic-to-cholesteric and cholesteric-to-smectic G* phase transitions were observed at 127.4°C and 82.2°C. The enthalpy value of the former was 0.64 J/g and the latter enthalpy value merged with the enthalpy value of crystal. Crystallization was observed at 80.9°C with an enthalpy value of 20.45 J/g.

DSC studies of LTA + 7BA reveal that the system is a di-phase variant. In the heating run two prominent transitions at 103.0°C and 121.6°C with enthalpy values of 48.27 and 3.88 J/g were attributed to crystal-to-melt and melt-to-cholesteric phases, respectively. The cholesteric-to-smectic G* phase was observed to be a monotropic transition in the heating run. In the cooling run the isotropic-to-cholesteric and cholesteric-to-smectic G* phase transitions were observed at 118.8°C with enthalpy value of 4.64 J/g and 116.1°C. Its enthalpy value merged with the enthalphy value of crystal. Crystallization was observed at 89.4°C with an enthalpy value of 45.01 J/g.

Phase Diagrams

The phase diagrams of pure p-n-alkoxy benzoic acids and the present homologous series (nBA + LTA) were constructed and reported [30] through optical polarizing microscopic studies by the phase transition temperatures observed in the cooling run. The textures observed are cholesteric (Ch; fingerprint texture) and smectic G* (multicolored mosaic texture) respectively. Figure 4 depicts the multicolored mosaic

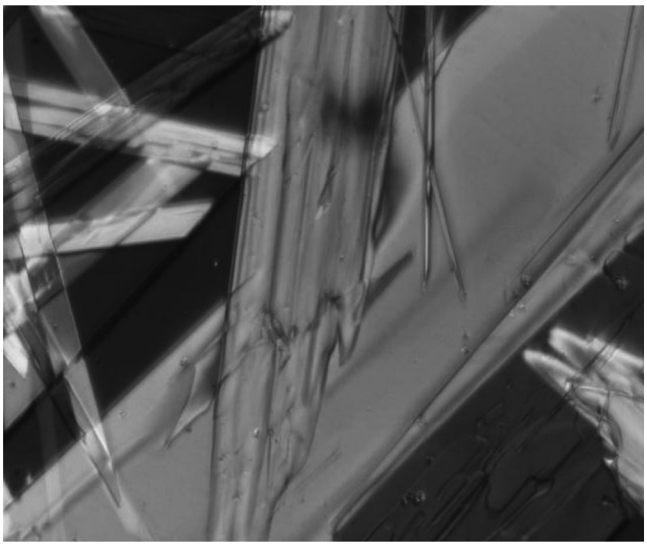

Figure 4. Texture of smectic G* phase of LTA + 8BA complex. Texture was digitally recorded with a magnification of 10×.

texture of smectic G* and Fig. 5 depicts the cholesteric texture. The phase diagram of pure p-n-alkoxy benzoic acids is reported [24] to exhibit three phases, namely, cholesteric, smectic C*, and smectic G*.

Phase Diagram of LTA + nBA Homologous Series

The phase diagram of LTA + nBA series is constructed from the DSC and optical polarizing microscopic studies and is depicted in Fig. 6. Phase transition

Figure 5. Texture of cholesteric phase in E_0 phase of LTA + 8BA. Texture was digitally recorded with a magnification of 10×.

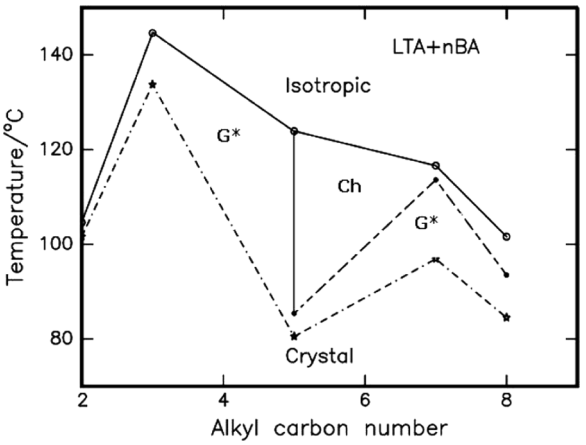

Figure 6. Phase diagram of LTA + nBA homologous series.

temperatures obtained by POM and DSC studies along with enthalpy values in J/g deduced from DSC studies for various homologous members of LTA + nBA are discussed in the previous section. The following points can be inferred from the phase diagram of the homologous series:

a. The lower homologous members, namely, LTA + 2BA and LTA + 3BA, are mono phase variant, exhibiting only the smectic G* phase, whereas the higher members, viz. LTA + 5BA, LTA + 7BA, and LTA + 8BA, are di-phase variant, and cholesteric and smectic G* phases are observed.
b. As the alkyl benzoic acid carbon number increased, it not only influenced the mesogenic thermal range from but also helped in inducement of a new phase namely, cholesteric.
c. Lower alkyl carbon numbers exhibit a mono phase variant, namely, smectic G*, whereas in the higher alkyl carbon numbers have di-phase variance with cholesteric and smectic G* phases.
d. The odd–even effect on mesogenic thermal range is observed in the present series. The mesogenic thermal range in the even compounds follows one trend and the odd compounds follows yet another trend of results. This effect is pronounced at the isotropic and crystallization temperatures of individual complexes.

Field Induced Transition (FiT)

It has been reported [29, 35–43] that when a mesogen is subjected to an applied external field in the cholesteric, nematic, or smectic C* phase, there can be a phase transition that is referred to as *field-induced transition* (FiT). The present hydrogen-bonded complexes are subjected to various strengths of external DC bias voltage derived from an HP 4192A impedance analyzer to investigate the occurrence of FiT.

Optical Shutter Action

LTA + 2BA and LTA + 3BA hydrogen-bonded complexes exhibit only a smectic G* phase; hence, optical shuttering action in the cholesteric phase is ruled out. In the

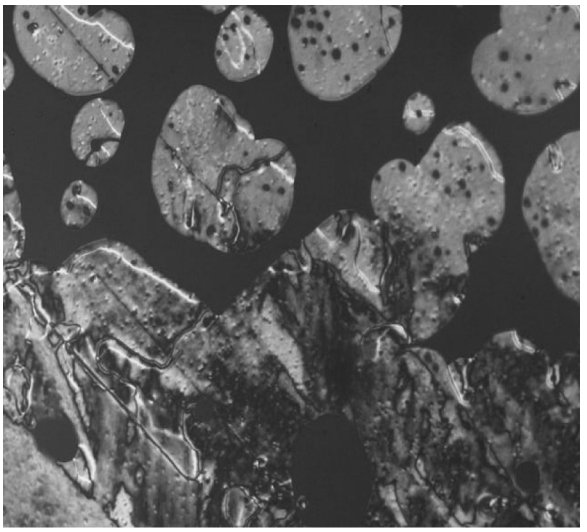

Figure 7. Texture of cholesteric phase in E_1 phase of LTA + 8BA. Texture was digitally recorded with a magnification of 10×.

other two members of the homologous series, namely, LTA + 5BA and LTA + 7BA, there is no effect of the field in the cholesteric phase of the corresponding mesogens.

The LTA + 8BA compound in its cholesteric phase when an applied DC bias voltage exceeds a particular threshold value, the phase of the compound is observed to prefer homeotropic like alignment with light being optically extinct, which is referred to as *optical shutter*. Figures 4, 5, and 7–9 depict the cholesteric texture under the influence of various applied field; further, it is interesting to note that immediately after withdrawing the bias voltage from any of the induced transitions,

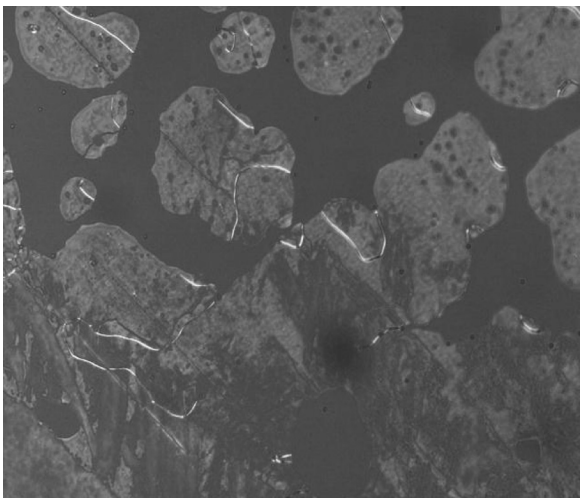

Figure 8. Texture of cholesteric phase in E_2 phase of LTA + 8BA. Texture was digitally recorded with a magnification of 10×.

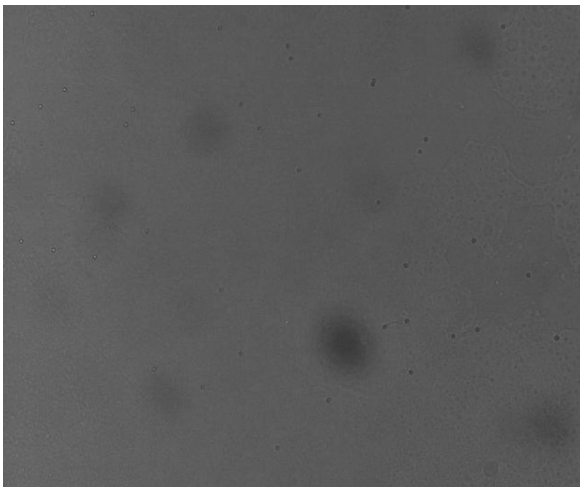

Figure 9. Texture of light extinction in optical shutter of LTA + 8BA. Texture was digitally recorded with a magnification of 10×.

the original texture of the cholesteric phase is retained. Thus, this process is reversible with bias voltage. In the entire thermal span of the cholesteric phase (~101°C to ~93°C) this is observed, whereas in the other phases preceding and succeeding cholesteric phase no such transition is found. Thus, the field-induced transitions can be represented as

$$E_0 \rightarrow E_1 \rightarrow E_2 \rightarrow \text{ Optical shutter}$$

The cholesteric phase with a bias voltage less than or equal to 1.25 v/μm is referred as E_0, where there is no change in the texture of the cholesteric phase as depicted in Fig. 5. When the field is increased beyond 1.25 v/μm the texture is completely changed (Fig. 7) and this phase is referred to as the E_1 phase. On further incrementing the field to 2.50 v/μm, the texture is again changed as shown in Fig. 8. This field-induced transition is refered as E_2.

An important observation is that when a DC bias voltage of 3.75 v/μm is applied, the optical extinction is observed with the optical texture of the compound suddenly becomes dark, this new phase is designated as optical shutter, which is depicted as Fig. 9. One of the possible reasons for this interesting phenomenon may be the realignment of the molecules to form a homeotropic-like alignment.

It is worth mentioning that similar results relating to field-induced transitions are obtained when a DC bias voltage of other polarity is applied.

To substantiate the above results, dielectric studies were performed. The variation of capacitance with respect to various external bias voltages was studied in cholesteric phase at two different frequencies, namely, 5 and 50 KHz. Such a variation for LTA + 8BA compound is shown in Fig. 10. The plot depicts a step-like variation of the capacitance with respect to applied bias voltages. From Fig. 10, it can be inferred that

a. field-induced transition, that is, $E_0 - E_1$, $E_1 - E_2$, E_2 – optical shutter are not sudden and abrupt but smooth and uniform.

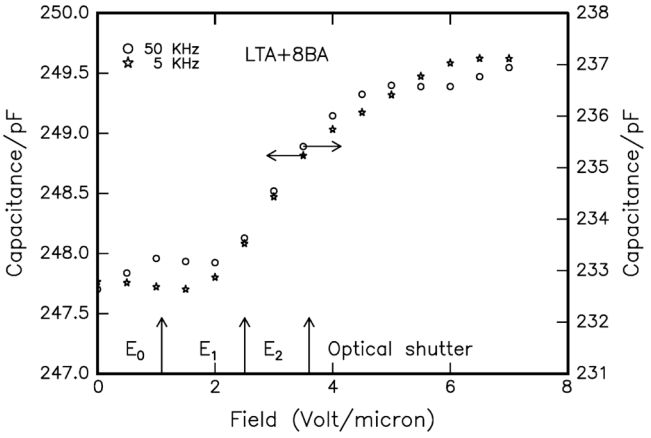

Figure 10. Capacitance variation of field in the cholesteric phase of LTA + 8BA.

b. frequency has no influence on the threshold values of the FiT.
c. at E_0 the capacitance remains unaltered and at the optical shutter the saturation of value of the capacitance is observed.
d. equilibrium states for the low and high fields are found to be distinct.

Intensity Profile of the Optical Texture in FiT

The sample LTA + 8BA was filled in a commercially available buffed cell (Instec (USA)) and silver leads were drawn for contact. The intensity profile in various phases was experimentally analyzed by applying external bias voltage of both polarities drawn from an impedance analyzer (HP 4192A (USA)) and the intensity of the light from the liquid-crystal sample was measured by a photo diode (TSL 252 (USA)) and $6^{1/2}$ digit multimeter (Keithley 2100 (Taiwan)). As the external bias voltage was incremented in small steps, this in turn induced various FiT at different magnitudes of the applied voltage. The variation of the intensity of the texture is noted at each step of the applied bias voltage and plotted as shown in Fig. 11. It is not surprising to note that the magnitude of the light is almost unaltered in any of the induced transitions except in E_0, E_1, and E_2. During the transition from E_0 to E_1 there is a steep, sudden decrement of the intensity of light manifesting the distortion of the helix. In the final phase of FiT, which is referred to as optical shutter, the optical profile is completely vanished. Thus, the liquid crystal behaved as an optical shutter (Figs. 4, 5, and 7–9). Hence, this HBLC may be used as a light modulator.

Qualitative Approach for Optical Shutter

A qualitative approach for the observed optical shutter phenomenon is described below. The distortion and change in the pitch of the cholesteric system with applied field in the liquid crystal mesogen is reported in the literature [44–49]. The change of the helical structure of a hydrogen-bonded liquid crystal (HBLC) in a thin-plane layer exposed to an external action (temperature or field) and its dependence on the molecular adhesive forces at the layer boundaries are responsible for field-induced transitions. If the helical pitch is not infinite, a nonzero average polarization

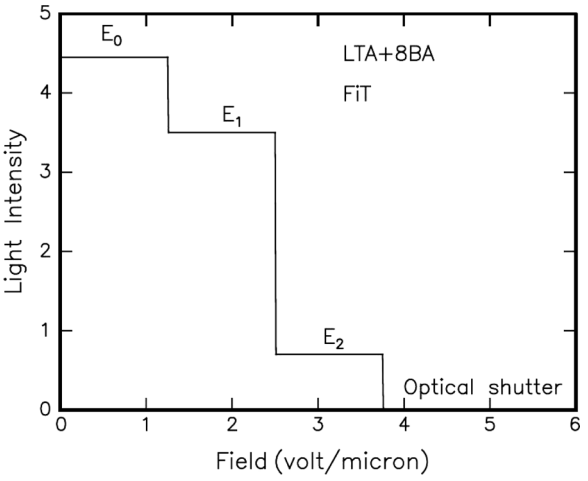

Figure 11. Intensity profile of the cholesteric phase under various applied external bias voltages.

exists locally. When subjected to weak electric fields, the helix distorts [41], giving rise to a small change in transmitted light as observed when the cell is placed under a crossed polarizer. At much stronger fields there is a sudden transition such that the azimuthal orientation of the director is spatially uniform and all layers polarization is parallel to the applied field.

LTA + 2BA and LTA + 3BA hydrogen-bonded complexes exhibit only the smectic G^* phase; hence, field-induced transitions in the cholesteric phase are ruled out. In the other two members of the homologous series, namely, LTA + 5BA and LTA + 7BA, there is no effect of field in the cholesteric phase of the corresponding mesogens.

Various FiTs observed in LTA + 8BA are discussed below with reference to optical textures (Figs. 4, 5, and 7–9), light intensity profile (Fig. 11), and molecular schematic representations (Fig. 12).

Field Induced Transition E_0 ($0 \leq 1.24$). When an applied stimulus is in the range of $0 \leq 1.24\,\text{v}/\mu\text{m}$, there is no apparent change in the texture of the cholesteric phase (Fig. 5) or in the light intensity profile. Figure 11 illustrates the unaltered light intensity profile, which indicates that in the entire electrical field region between 0 to $1.24\,\text{v}/\mu\text{m}$ it gives rise to molecular orientation depicted in Fig. 12. Because the texture (Fig. 5) and light intensity profile (Fig. 11) are unaltered in this entire field, it is referred as E_0. The plane of the molecules lies parallel to plane of the liquid-crystal cell and a continuous variation of the director orientation with field ($E = 0$) begins; thus, the director profile is undisturbed, which is as shown in Fig. 11.

Field Induced Transition E_1 ($1.25 \geq 2.49$). When the external stimulus is between 1.25 to $2.49\,\text{v}/\mu\text{m}$, the texture of the cholesteric phase changes as depicted in Fig. 7. There is a sudden decrement in the magnitude of the light intensity profile. It is worth mentioning that both these parameters remain unaltered throughout this external field. The molecules rotate to an angle as shown in Fig. 12. At this level, the electric field is sufficient to overcome the elasticity possessed by the

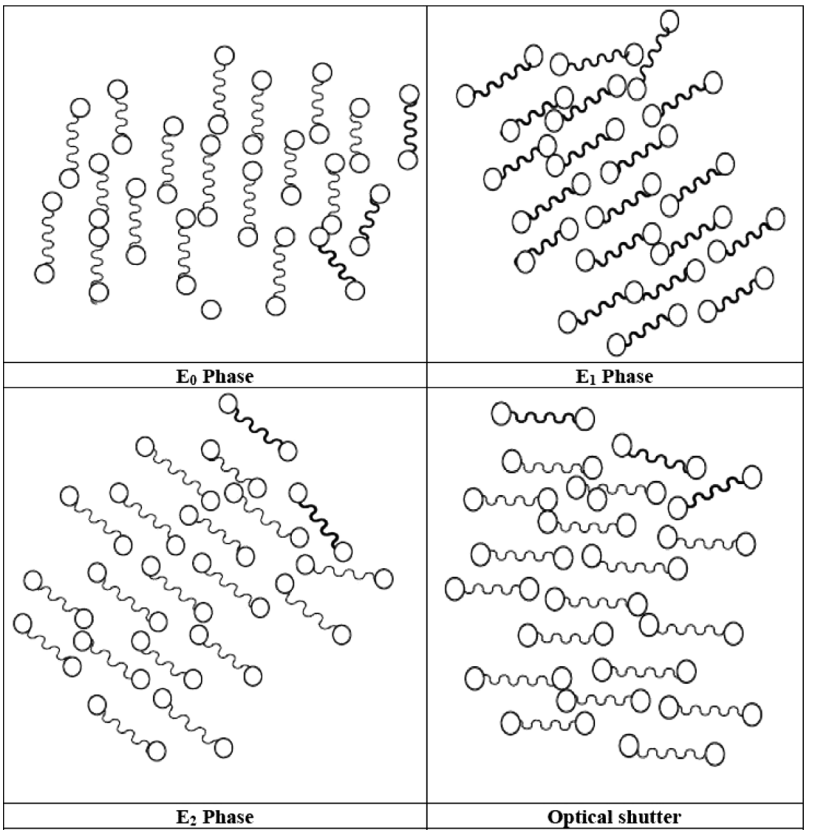

Figure 12. Schematic representation for the field-induced transitions of LTA + 8BA. Arrangement of molecules in various field-induced transitions, namely, E_0, E_1, E_2, and optical shutter are depicted.

molecules. Molecules in the adjacent layer undergo unequal azimuthal rotations, resulting in change of the helical pitch.

Field Induced Transition E_2 ($2.50 \geq 3.74$). As the field is increased to 2.50 v/μm, a phase transition is observed, which is designated as E_2, and the corresponding texture is shown as Fig. 8. The steep jump in the magnitude of the light intensity, toward the lower side (Fig. 11), is attributed to this phase change. The molecular orientation for this phase is as shown in Fig. 12. In this phase the distortion of the helicoidal pitch is greater and, in turn, rapid switching is observed, which is analogous to short helical pitch materials.

Field Induced Transition OS (≥ 3.75). An interesting feature is observed when the magnitude of the field reaches a threshold value of 3.75 v/μm. The liquid-crystal material behaves as an optical shutter, as can be observed from the light intensity profile (Fig. 11). The optical extension has been recorded by the optical textural study, which is depicted as Fig. 9. This phase is referred to as optical shutter. It is no surprise that the molecules prefer an alignment that resembles homeotropic alignment (Fig. 12). When the external field is increased to a threshold value of

3.75 v/μm, the molecules inhibit the light and act as a total optical shutter. The possible reasons for this field-induced transition can be elicited from the various surface anchoring energy [49] possessed by the liquid-crystalline molecules.

Conclusions

a. A novel hydrogen-bonded ferroelectric liquid-crystal series was synthesized and characterized.
b. The formation of a hydrogen bond was confirmed by FTIR measurements.
c. A detailed analysis of various field-induced transitions in the cholesteric phase of the hydrogen-bonded complex was performed.
d. Dielectric data, optical studies, and intensity measurements supported the observed field-induced transitions.

Acknowledgment

M. L. N. Madhu Mohan acknowledges the financial support rendered by the All India Council for Technical Education (AICTE), Department of Science and Technology (DST), and Defence Research Development Organization (DRDO), New Delhi. Infrastructural support provided by the Bannari Amman Institute of Technology is gratefully acknowledged.

References

[1] Meyer, R. B., Liebert, L., Strezelecki, L., & Keller, P. (1975). *J. Physique. Lett.*, *30*, 69.
[2] Kato, T. (1998). *Handbook of Liquid Crystals*, Wiley-VCH: Weinheim.
[3] Gray, G. W. (1962). *Molecular Structure and Properties of Liquid Crystals*, Academic Press: London.
[4] Kelker, H., & Hatz, R. (1980). *Handbook of Liquid Crystals*, Verlag Chemie: Weinheim.
[5] Kato, T., & Frechet, J. M. J. (1993). *J. Am. Chem. Soc.*, *111*, 8533.
[6] Yu, L. (1993). *Liq. Cryst.*, *14*, 1303.
[7] Kato, T., Kihara, H., Uryu, T., Ujiie, S., Iimura, K., Fréchet, J. M. J., & Kumar, U. (1993). *Ferroelectrics*, *148*, 161.
[8] Kato, T., Uryu, T., Kaneuchi, F., Jin, C., & Fréchet, J. M. J. (1993). *Liq. Cryst.*, *14*, 1311.
[9] Demus, D., Demus, H., & Zaschke, H. (1974). *Flussige Kristalle Tabellen*, VEB Deutcher Verlag fur Grundstoffindustrie: Leipzig.
[10] Paleos, C. M., & Tsiourvas, D. (2001). *Liq. Cryst.*, *28*, 1127.
[11] Xu, B., & Swager, T. M. (1995). *J. Am. Chem. Soc.*, *117*, 5011.
[12] Malik, S., Dhal, P. K., & Mashelkar, R. A. (1995). *Macromolecules*, *28*, 2159.
[13] Sideratou, Z., Tsiourvas, D., Paleos, C. M., & Skoulios, A. (1997). *Liq. Cryst.*, *22*, 51.
[14] Goodby, J. W., Blinc, R., Clark, N. A., Lagerwall, S. T., Osipov, S. A., Pikin, S. A., Sakurai, T., Yoshino, Y., & Zecks, B. (1991). *Ferro Electric Liquid Crystal, Principles, Properties, and Applications*, Gordon & Breach Press: Philadelphia.
[15] Clark, N. A., & Lagerwall, S. T. (1980). *Appl. Phys. Lett.*, *36*, 899.
[16] Vijayakumar, V. N., & Madhu Mohan, M. L. N. (2009). *Solid State Commun.*, *149*, 2090.
[17] Vijayakumar, V. N., & Madhu Mohan, M. L. N. (2009). *Braz. J. Phys.*, *39*, 600.
[18] Kumar, P. A., Srinivasulu, M., & Pisipati, V. G. K. M. (1999). *Liq. Cryst.*, *26*, 859.
[19] Swathi, P., Kumar, P. A., & Pisipati, V. G. K. M. (2000). *Liq. Cryst.*, *27*, 665.
[20] Srinivasulu, M., Satyanarayana, P. V. V., Kumar, P. A., & Pisipati, V. G. K. M. (2001). *Liq. Cryst.*, *28*, 1321.

[21] Swathi, P., Sreehari Sastry, S., Kumar, P. A., & Pisipati, V. G. K. M. (2001). *Mol. Cryst. Liq. Cryst.*, *365*, 523.
[22] Sreedevi, B., Chalapathi, P. V., Srinivasulu, M., Pisipati, V. G. K. M., & Potukuchi, D. M. (2004). *Liq. Cryst.*, *31*, 303.
[23] Chitravel, T., Madhu Mohan, M. L. N., & Krishnakumar, V. (2008). *Mol. Cryst. Liq. Cryst.*, *493*, 17.
[24] Vijayakumar, V. N., Murugadass, K., & Madhu Mohan, M. L. N. (2009). *Mol. Cryst. Liq. Cryst.*, *515*, 37.
[25] (a) Madhu Mohan, M. L. N., Arunachalam, B., & Arravindh Sankar, C. (2008). *Metal and Mater. Trans. A*, *39*, 1192; (b) Madhu Mohan, M. L. N., & Arunachalam, B. (2008). *Z. Naturforch*, *63a*, 435.
[26] Madhu Mohan, M. L. N., & Pisipati, V. G. K. M. (2000). *Liq. Cryst.*, *26*, 1609.
[27] (a) Kumar, P. A., Madhu Mohan, M. L. N., & Pisipati, V. G. K. M. (2000). *Liq. Crys.*, *27*, 1533; (b) Vijayakumar, V. N., & Madhu Mohan, M. L. N. (2009). *Braz. J. Phys.*, *39*, 4 (in press) (2010).
[28] Madhu Mohan, M. L. N., Kumar, P. A., Goud, B. V. S., & Pisipati, V. G. K. M. (1999). *Mater. Res. Bull.*, *34*, 2167.
[29] (a) Madhu Mohan, M. L. N., Kumar, P. A., & Pisipati, V. G. K. M. (1999). *Ferroelectrics*, *227*, 105; (b) Vijayakumar, V. N., Murugadoss, K., & Madhu Mohan, M. L. N. (2010). *Mol. Cryst. Liq. Cryst.*, *517*, 41.
[30] Vijayakumar, V. N., & Madhu Mohan, M. L. N. (2009). *Integrated Ferroelectrics*, *392*, 81.
[31] Gray, G. W., & Goodby, J. W. G. (1984). *Smetic Liquid Crystals Textures and Structures*, Leonard Hill: London.
[32] Kumar, S. (2001). *Liquid Crystals: Experimental Study of Physical Properties and Phase Transitions*, Cambridge Press: Cambridge.
[33] de Gennes, P. G. (1974). *The Physics of Liquid Crystals*, Oxford Press: London.
[34] Stanley, H. E. (1971). *Introduction to Phase Transition and Critical Phenomena*, Clarendon Press.
[35] Kobayashi, S., & Ishibashi, S. (1994). *Mol. Cryst. Liq. Cryst.*, *257*, 181.
[36] Jong-Guang, W., & Shu-Hsia, C. (1994). *Jap. J. Appl. Phys.*, *33*, 6249.
[37] Qian, T., & Taylor, P. L. (1999). *Phys. Rev. E*, *60*, 2978.
[38] Napoli, G. (2006). *J Appl. Maths.*, *71*, 34.
[39] Schlangen, L. J. M., Alexandre, P., & Cornelissen, H. J. (2000). *J. Appl. Phys.*, *87*, 3723.
[40] Hurd, A. J., Fraden, S., Lonberg, F., & Meyer, R. B. (1985). *J. de Physique*, *46*, 905.
[41] Zhang, S., Wen, B., Keast, S. S., Neubert, M. E., Taylor, P. L., & Rosenblatt, C. (2000). *Phys. Rev. Lett.*, *84*, 4140.
[42] Rotinyan, T. A., Ryumtsev, E. I., & Yazikov, S. B. (1987). *JETP Lett.*, *46*, 417.
[43] Cladiss, P. E., Garel, T., & Pieranski, P. (1986). *Phys. Rev. Lett.*, *57*, 2841.
[44] Abdulhalim, I., & Moddel, G. (1991). *Mol. Cryst. Liq. Cryst.*, *200*, 79.
[45] Judge, L. A., Kriezis, E. E., & Elston, S. J. (2001). *Mol. Cryst. Liq. Cryst.*, *366*, 661.
[46] Schiller, P., & Zeitler, J. (1997). *Phys. Rev. E*, *56*, 531.
[47] Schiller, P., & Zeitler, J. (1995). *de Physique II*, *5*, 1835.
[48] Petit, M., Daoudi, A., Ismaili, M., & Buisine, J. M. (2006). *Euro. Phys. J. E*, *20*, 27.
[49] Indekeu, J. O., & Berker, A. N. (1986). *Phys. Rev. A*, *33*, 1158.